LIGHT OPTICS FOR OPTICAL STOCHASTIC COOLING*

M. B. Andorf[1], J. Ruan[2] V. A. Lebedev[2] and P. Piot[1,2]
[1] Department of Physics and Northern Illinois Center for Accelerator & Detector Development, Northern Illinois University DeKalb, IL 60115, USA
[2] Fermi National Accelerator Laboratory, Batavia IL 60510, USA

Abstract

In Optical Stochastic Cooling (OSC) radiation generated by a particle in a "pickup" undulator is amplified and transported to a downstream "kicker" undulator where it interacts with the same particle which radiated it. Fermilab plans to carry out both passive (no optical amplifier) and active (optical amplifier) tests of OSC at the Integrable Optics Test Accelerator (IOTA) currently in construction [1]. The performance of the optical system is analyzed with simulations in Synchrotron Radiation Workshop (SRW) accounting for the specific temporal and spectral properties of undulator radiation and being augmented to include dispersion of lens material.

INTRODUCTION & DESIGN CONSIDERATION

A proof-of-principal experiment on Optical Stochastic Cooling (OSC) is planned at the Integrable Optics Test Accelerator (IOTA) currently in construction at Fermilab. OSC is a technique for beam cooling capable of achieving damping rates orders of magnitude faster than microwave stochastic cooling and thus provides a way to achieve higher luminosities in future hadron colliders [2, 3].

To reduce cost the OSC in IOTA will be demonstrated with an electron beam. It is planned to be carried out in two phases. The first phase will be based on a passive scheme in which light from the pickup is just focused into the kicker. The second phase will include a single-pass optical amplifier based on a Cr:ZnSe [4]. This paper focuses on the passive scheme with base wavelength of the undulator, 2.2 μm chosen to be within the amplifier medium band. The beam optics was designed to achieve both transverse and longitudinal cooling. General details of OSC can be found in [5].

To maximize cooling rates the light optics should be chosen so that the transfer matrix between centers of the pickup and kicker be equal to the identity matrix or its negative $\pm\mathbf{I}$. The choice of negative matrix is preferred because it results in weaker focusing (and consequently reduced focusing chromaticity) and is a better match to the pickup to kicker transfer matrix. The latter results in that a particle radiating with a positive (resp. negative) transverse offset in the pickup meets its radiation with a negative (resp. positive) offset in the kicker. The minimum number of lenses required to obtain $\pm\mathbf{I}$ is equal to 3. In the case of the $-\mathbf{I}$ transformation, the focal lengths and locations of the lenses (see Figure 1) are:

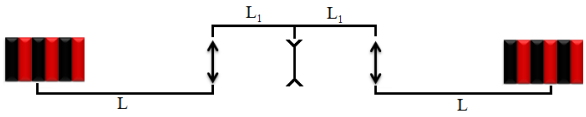

Figure 1: Optical transport line between the pickup and kicker undulators with associated three-lens telescope.

$$F_1 = L_1, \text{ and } \quad F_2 = -\frac{L_1^2}{2(L-L_1)}. \tag{1}$$

The total length from pickup to kicker is $2(L+L_1)$. Lowering the focusing (and so chromaticity) requires L_1 to be as large as permissible. Ultimately the drift L_1 is constrained by the length of the chicane separating the beam and its radiation on the way from pickup to kicker.

Table 1: Specifications for the Passive-OSC Telescope Diagrammed in Fig. 1

parameter	value	unit
L_1, F_1	1.35	m
F_2	-4.2	cm
Half-Aperture	7	mm
Material	BaF_2	-
Total Delay, Δs	2	mm

Table 1 summarizes the main parameters of the telescope used in the simulations presented below. Figure 2 shows the radiation fields in the kicker in the absence of dispersion. These parameters can be somewhat adjusted with advances in the design of the OSC straight. Barium Fluoride (BaF_2) was selected as material for optics lenses due to its low group velocity dispersion (GVD) of 9.74 fs^2/mm [6].

Synchrotron Radiation Workshop (SRW) [7] was used for the numerical simulations of the light optics for OSC. It allows one to simulate the generation of radiation by a single electron passing through the pickup undulator and radiation propagation and focusing to the kicker. Because of the large operating bandwidth ($\lambda \in [2.2 - 2.9]$ μm), SRW had to be extended to properly account for dispersion as detailed in the next section.

INCLUDING CHROMATIC EFFECTS

SRW includes several optical components commonly used in X-ray optics such as compound refractive lenses (CRV),

* Work supported by the by the US Department of Energy (DOE) contract DE-SC0013761 to Northern Illinois University. Fermilab is operated by the Fermi research alliance LLC under US DOE contract DE-AC02-07CH11359.

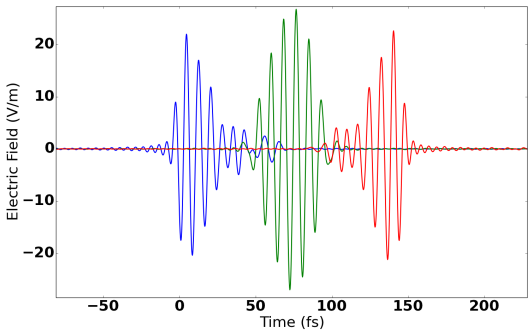

Figure 2: On-axis undulator radiation pulses emitted from the pickup and being observed at the front (red), center (green) and back (blue) of the kicker undulator (dispersion in the optical system is not included). An artificial delay has been added to the pulses for clarity. Small amplitude oscillations observed before and after pulses are due to finite resolution of Fast Fourier Transform.

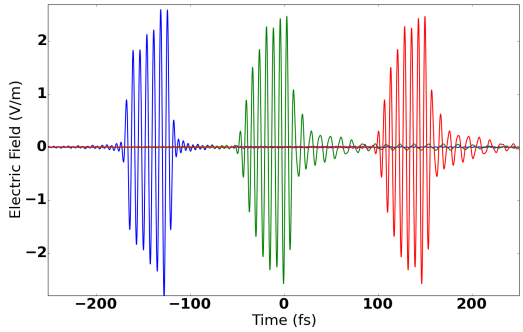

Figure 3: On-axis undulator radiation just upstream of the first lens (blue), its modification downstream passing through a 5-mm slab of BaF_2 using the implemented SRW model (green) and computed from Eq.4 (red). An artificial delay has been added to the pulses for clarity.

thin ideal lenses, mirrors and apertures. However in the OSC setup being studied thick conventional lenses are employed. This type of component exhibits the behavior of real glass including first and second order dispersions. Therefore we augmented SRW with our own routines by extending the model already implemented in SRW. We especially introduced, given a specified lens profile (in our case a planoconvex or planoconcave), the path length of the optical rays as a function of transverse offset and photon energy. In addition to the lens profile, the path length at a given photon energy (or wavelength) is found by calculating the index of refraction, n, at this energy.

Most glasses in the visible and mid-IR regimes are well studied and can be described using the Sellmeier's empirical equation to give $n(\lambda)$. The specific form of Sellmeier's equation depends on the component of interest but generally has the form:

$$n(\lambda) = \sqrt{1 + \sum_j \frac{A_j \lambda^2}{\lambda^2 - B_j}}, \tag{2}$$

with A_j and B_j empirically determined coefficients and usually the summation is limited to $j = 0,\ 1,\ 2$. For our telescope $\lambda_s = 2.2\ \mu$m is taken to be the on-axis undulator-radiation wavelength and correspondingly $n(\lambda_s) = 1.4641$ for BaF_2 [6]. Differentiation of Eq. 2 provides the dispersion $(dn/d\lambda)$ and GVD $(d^2n/d\lambda^2)$ for the glass of interest to high precision. The lens focal length, f, is directly obtained from the lens maker equation which in vacuum is

$$\frac{1}{f(\lambda)} = \frac{n(\lambda) - 1}{R}, \tag{3}$$

where R is the radius of curvature of the lens. From Eq. 3 the first order effect is clearly evident given the explicit focal length dependency on wavelength.

The effect of GVD lengthens the pulse and induces a chirp. We can observe these effects by passing the undulator radiation through a thick slab of material. The spectrum of electromagnetic wave passing through a dispersive material of thickness z is modified according to: [9]

$$E(\omega, z) \quad = \quad E(\omega) \exp(ikz) \tag{4}$$

with $k \equiv 2\pi n/\lambda$ being the wavevector. To quantify our extension to SRW we compute the correlation function between the field directly obtained from Eq. 4, $E_1(t)$, and simulated with the model implemented in SRW, $E_2(t)$,

$$\gamma_{12}(\tau) = \frac{\langle E_1(t) E_2^*(t+\tau)\rangle}{\left[\langle |E_1|^2\rangle \langle |E_2|^2\rangle\right]^{1/2}}. \tag{5}$$

We considered the E-field associated to the undulator radiation after it has passed through a 5-mm thick BaF_2 slab. The correlation function has a maximum value greater than $\max(\gamma_{12}) > 0.999$; see also Fig. 3. Such a value gives confidence in our numerical implementation of the thick lens.

ELECTRON KICK

Interaction of an electron with its radiation in the kicker undulator results in the energy change equal to:

$$\Delta E = q \int \mathbf{E}.\mathbf{v} dt \simeq q \int E_x v_x dt, \tag{6}$$

with q the electron charge and $v_x = \frac{\beta c K}{\gamma} sin(\frac{2\pi z}{\lambda_p})$ the transverse electron velocity [10]. In order to find the field E_x experienced by an electron, one must account for the slippage that occurs between the light wave moving with the speed of light and the electron moving with an average velocity $\bar{\beta} = \beta(1 - \frac{1}{4}\frac{K^2}{\gamma^2})$ in units of c. For simplicity integration of Eq. 6 is replaced by summing with a time step, $\delta z_l / c\bar{\beta}$ that results in a slippage between the light wave and electron

ISBN 978-3-95450-147-2

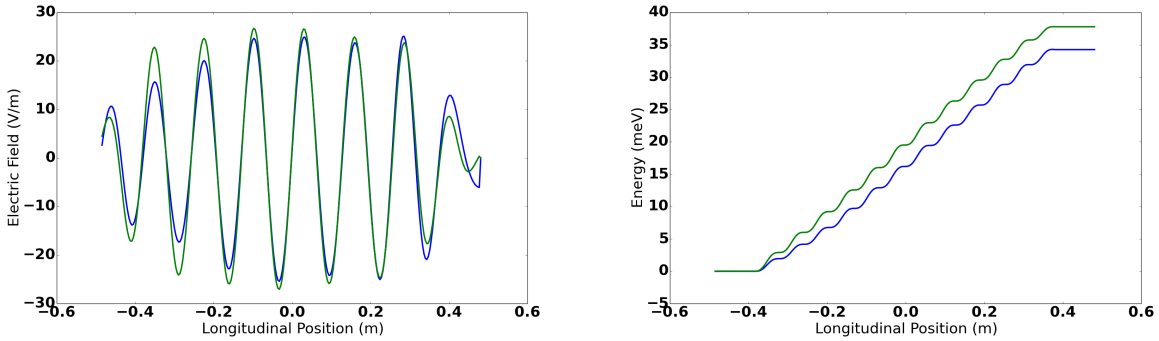

Figure 4: Left: Electric field experienced by an electron in the kicker undulator with (blue) and without (green) dispersion (green). Right: Energy transfer from the radiation field to the electron integrated over the kicker-undulator length for a phase corresponding to the maximum kick.

Table 2: Undulator Parameters used in Simulations

parameter	value	unit
Peak B field	664	G
Undulator parameter K	0.79	-
Undulator period, λ_p	12.83	cm
Undulator length, L_u	77	cm
center wavelength, λ_s	2.2	μm
Beam Energy, E	100	MeV

equal to the time resolution, δt_f, of our fields corresponding to the coordinate transform

$$\delta z_l = c\frac{\delta t_f}{1-\bar{\beta}}. \tag{7}$$

Figure. 4 (left plot) presents the field experienced by an electron as it slips co-propagating with the pickup radiation in the kicker undulator; the undulator parameters are given in 2. In the case of perfect focusing of all wavelengths by the described above lens telescope the particle sees an electric field with constant amplitude along the entire length of the undulator with a period equal to its motion in the kicker. When dispersion is included the amplitude decreases slightly for light imaged at the front of the kicker.

From the computed electric field and the electron velocity as a function of time using $z = \bar{\beta}ct$, Eq. 6 can be numerically integrated. We find that in the absence of dispersion the amplitude of the kick is $\Delta E \simeq 38$ meV while including dispersion in the radiation transport reduces the kick to $\Delta E \simeq 34$ meV.

Note that this analysis does not include (i) the longitudinal oscillations of the electron around its average velocity in the kicker and (ii) the transverse dependence on field strength of the radiation. For the undulator parameters considered here, the amplitude of the longitudinal oscillations is $\frac{K^2\lambda_p}{16\gamma^2\pi} \simeq 41$ nm and is negligible compared to λ_s. The transverse amplitude $\frac{K\lambda_p}{2\pi\gamma} = 83\ \mu$m is on the same order of the radiation spot size and will thus lead to a reduction in effective kick.

In [5] an expression for the kick amplitude is derived under the assumption of $K \ll 1$, which in practical units can be written as

$$\Delta E\ [\text{meV}] = 1.451\frac{E^2[\text{MeV}]K^2L_u[\text{m}]}{\lambda_p^2[cm]}f_L(\gamma\theta) \tag{8}$$

with $f_L(x) = 1 - \frac{1}{(1+x^2)^3}$ accounting for the finite transverse acceptance of the telescope. For our beam energy, lens radius and distance from the pickup center, $f_L = 0.88$. The above equation yields a kick amplitude of 37 meV in close agreement with the value simulated earlier.

Using the thin lens approximation for the particle beam optics and theory developed in [5] we can estimate the damping time for the longitudinal and horizontal phase spaces respectively as

$$\tau_s = \frac{c\kappa(2\Delta s - \Phi D^* h)}{2C}, \text{ and } \tau_x = \frac{c\kappa\Phi D^* h}{2C}. \tag{9}$$

Here $\kappa \equiv \frac{2\pi}{\lambda_s}\frac{\Delta E}{E}$, $\Phi \approx 14\ \text{cm}^{-1}$ is the strength of the quadrupole in the chicane center, $D^* \approx 50$ cm is the dispersion in the chicane center, $h \approx 35$ mm is the horizontal offset of the beam and $C = 40$ m is the circumference of IOTA. With the above values we estimate $\tau_s = 6\ \text{s}^{-1}$ and $\tau_x = 9\ \text{s}^{-1}$.

CONCLUSION AND FUTURE WORK

Using SRW with our own routines for accounting for chromatic effects we were able to compute the kick an electron receives during a single pass through the OSC section. In the absence of dispersion the value we calculate is close to the analytic formulas given in [5]. When we include dispersion of the lens material the kick decreases by roughly 10 %.

The work presented here improved our understanding of the pick-up radiation distribution in the kicker location and verified results of analytic theory. It also assured us that a transition to higher K undulator is advantageous. We expect Increasing K from 0.79 to about 1 will yield almost a factor of 2 increase in the kick amplitude. Further increase will reduce an interaction with the electromagnetic wave due to

increased transverse separation of particle and its radiation in the kicker undulator.

REFERENCES

[1] V. Lebedev, et al., Proc. COOL'15 (in press, 2015)

[2] A.A.Mikhailichkenko, M.S. Zolotorev Phys. Rev. Lett. (71),(25), p.4146. (1993)

[3] M. S. Zolotorev, A. A. Zholents Phys. Rev. E, 50, 4, p.3087. (1994)

[4] M. B. Andorf, et al., Proc. IPAC15, Richmond, VA, p.659. (2015).

[5] V.A. Lebedev, "Optical Stochastic Cooling," ICFA Beam Dyn. Newslett. **65** 100 (2014).

[6] M. N. Polyanskiy. "Refractive index database," http://refractiveindex.info

[7] O. Chubar, P. Elleaume, Proc. EPAC98, Stockholm Sweden, p.1177 (1998).

[8] W. Sellmeier, Ann. Phys. Chem. 219 (6), 272 (1871)

[9] A.E. Siegman, *Lasers*, University Science Books (1986)

[10] H. Wiedemann, *Particle Accelerator Physics* 3rd ed. Springer (2007)

ISBN 978-3-95450-147-2